MEDWIN PUBLISHERS
Committed to Create Value for Researchers

Open Access Journal of Astronomy
ISSN :2996-6701

Structural, Optical and Magnetic Investigations on Pure and Copper Doped ZnO@ZnS Core Shell Nanoparticles for Biological Applications

SivaSankari J*, Nivethaa EAK and Naseeha EMH

Department of Physics, B.S. Abdur Rahman Crescent Institute of science and Technology, India

***Corresponding author:** SivaSankari J, Department of physics, B.S. Abdur Rahman Crescent Institute of science and Technology, Vandalur, Chennai 600048, India, Email: sivasankari@crescent.education

Research Article

Volume 2 Issue 2

Received Date: October 08, 2024

Published Date: November 05, 2024

DOI: 10.23880/oaja-16000137

Abstract

ZnO nanoparticles were synthesized by co-precipitation with no capping agent followed by covering with ZnS using a solution-based chemical method at low temperature. By varying the solution concentration, it was found that the fully-covering ZnS shell forms by a reaction of Na_2S with ZnO NPs followed by the formation of ZnS nano-crystals by the reaction of Na2S with $ZnCl_2$. The mechanism that led to full coverage of the ZnO core is proposed to be the addition of $ZnCl_2$ at a later stage of the growth which guarantees a continuous supply of Zn ions to the core surface. Moreover, the ZnS nano- crystals that uniformly cover the ZnO NPs show no epitaxial relationship between the ZnO core and ZnS shell. The slow atomic mobility at the low reaction temperature is attributed to the non-epitaxial uniform ZnS shell growth. The rough surface of the ZnO grains provides initial nucleation positions for the growth of the ZnS shell nano-crystals. The low growth temperature also inhibits the abnormal growth of ZnS grains and results in the homogeneous coverage of ZnS nano-crystals on the ZnO core surface. The morphology and structure of samples are verified by X-ray diffraction (XRD). Identification of unknown substances and quantitative analysis can be done by FTIR. The absorption and reflectance of the nanoparticles were analyzed by UV Visible spectroscopy.

Keywords: ZnO @ZnS; Core Shell Nanoparticles; Microstrain; Pl; FTIR; Biological Application

Abbreviations

CSNP: Core Shell Nano Particles; XRD: X-ray Diffraction; NPs: Nanoparticles; SAED: Selected Area Electron Diffraction; NBE: Near-Band- Edge; PL: Photo Luminescence; ROS: Reactive Oxygen Species; FT-IR: Fourier Transform Infrared; ZnO: Zinc Oxide.

Introduction

Over the years, nanotechnology has attracted a lot of interest where its essential component is nanoparticles. Nanoparticles are made up of Carbon, metals, metal oxides or organic matters and exhibit unique physical, chemical, optical and biological properties at nanoscale when compared to the corresponding bulk materials. This phenomenon might be due to increased reactivity, surface area to the volume, stability and enhanced mechanical strengths. Apart from their chemical composition, the nanoparticles may vary in size, shape, and dimensions. Nanoparticles can be of zero dimensional such as nano dots where length, width, height are all fixed in single axis. They can also be of 1D such as Graphene where it may have one parameter, 2D such as Carbon nanotubes where it has both length and breadth

and 3D like gold nanoparticles where it has all the three parameters [1]. The creation and properties of quantum dots, or nanoparticles, have received a lot of interest in the last ten years. Small particles with a diameter of 1–100 nm are known as nanoparticles or quantum dots. The optical properties start to alter when the particle diameter gets closer to its Bohr diameter, and the quantum confinement effect becomes much more significant. As a result, bulk materials and nanoscale-scale particles have very different physical and electrical characteristics [2]. One of the most fascinating and cutting-edge techniques for consistently and successfully synthesizing flexible nanostructure materials is surface modification.

Because of their adaptable frameworks and qualities, core-shell composite materials have attracted a lot of interest for a wide range of important applications [3]. The quantum confinement effect, which is the spatial three-dimensional confinement of electrons and holes in a compact box, controls the physical and chemical properties of semiconductor nanoparticles (NPs). When the nanoparticle size is near the exciton Bohr radius, the quantum confinement effect causes a noticeable rise in the band-gap and a blue shift in the absorption spectra. The effects of size on the luminous characteristics of the nanostructures are analyzed using the effective mass model. The optical characteristics of the nanoparticles encased in a shell coating layer were found to be enhanced. Because of its large exciton binding energy of 60 meV and wide band gap of 3.3 eV at room temperature, zinc oxide (ZnO) is one of the most well-known II–VI semiconductor nanoparticles. It is used in a wide range of applications, including optoelectronics, field-effect transistors, sensors, transparent conducting films, light-emitting diodes, and catalysts as it is very cheap and non-toxic semiconductor. There are reports that encapsulating ZnO with large pore sizes can greatly enhance the optical characteristics of ZnO NPs. There are two naturally occurring phases of zinc sulfide (ZnS): the zinc mix structure, which has a cubic phase, and the wurtzite structure, which has a hexagonal phase. ZnS is a non-toxic semiconductor with a wide and straight band gap. The bulk cubic and hexagonal phases of zinc sulfide have band-gap energies of 3.68 eV and 3.80 eV, respectively [5]. At lower temperatures and air pressures, zinc blend ZnS is more stable; nonetheless, at temperatures exceeding 1000 °C, it changes into wurtzite ZnS. It has been reported recently that ZnS QDs exhibit a variety of luminescence features, including photo-, electro-, mechano-, and thermal-luminescence [6,7]. Because of their broad excit on binding energy of 40 meV, ZnS QDs, another phosphor material, are widely employed in LEDs, flat- panel displays, and infrared windows. It is found that, ZnS nanoparticles (NPs) is an excellent shell coating layer on the ZnO, and enhances the optical properties of the ZnO–ZnS core–shell nanostructures (Figure 1). Investigations are conducted into how ZnO–ZnS core–shell nanostructures optical characteristics are affected by their thickness. By controlling the proportion of Na_2S, the sulfur source in the hydrothermal process, the shell thickness and optical characteristics of the ZnO–ZnS core–shell nanostructures were controlled. The NaOH treatment as a capping agent for ZnS QD production is also thoroughly examined [8]. The diagrams representing the formation of ZnO/ZnS and ZnO: Cu/ZnScore-shell nanoparticles are shown below Figure 1 & 2:

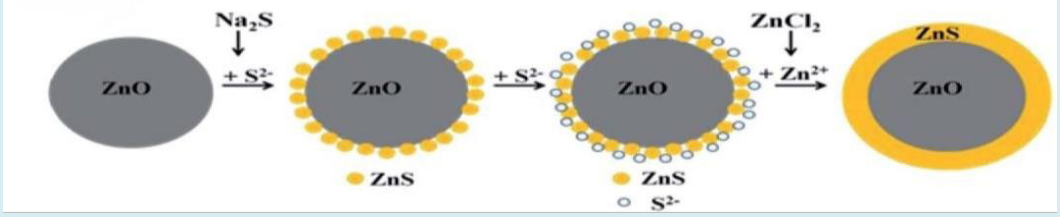

Figure 1: ZnO@ZnS core-shell nanoparticle.

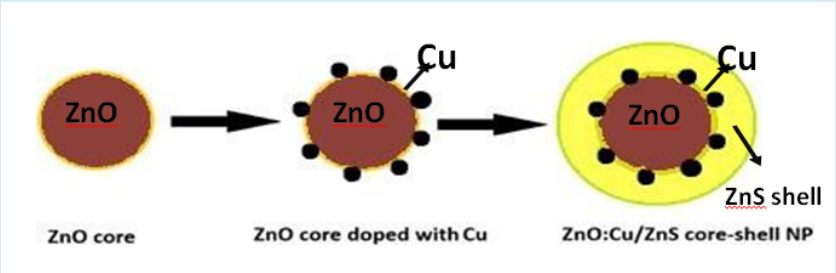

Figure 2: ZnO: Cu@ZnS core-shell nanoparticle.

Experimental Method

Synthesis of Pure ZnO/ZnS Core-Shell Nanoparticles by Co-Precipitation Method

- **STEP 1:** For the synthesis of pure form of ZnO/ZnS core-shell nanoparticles, 100g of Zinc oxide (ZnO) is mixed with 50ml of Isopropanol (C_3H_8O) and the mixture is stirred with the help of a magnetic stirrer for about one hour at room temperature where the solution is found to be saturated.
- **STEP 2:** Simultaneously, about 1.5g of Sodium sulfide (Na_2S) is added to 200ml of distilled water and stirred using a magnetic stirrer for 30 minutes at room temperature.
- **STEP 3:** Once they are done stirring, mix the above two solutions in a 1000ml beaker and allow them to stir for 1 hour at room temperature.
- **STEP 4:** Now, about 0.6815g of Zinc chloride ($ZnCl_2$) is added to a 100ml beaker containing 50ml of distilled water. $ZnCl_2$ is allowed to dissolve completely.
- **STEP 5:** After an hour of continuous stirring of above two mixtures, zinc chloride solution is added dropwise with the help of a filler. Now, the solution mixture containing $ZnCl_2$ is allowed to stir for 3 to 4 hours with the temperature being maintained at 80°C.
- **STEP 6:** Once the continuous stirring is done for 3-4 hours. The beaker containing the solution is covered with an aluminium foil with holes poked on it. The solution beaker is then kept undisturbed for about 12 to 15 hours. By isolating the solution, the so formed ZnO/ZnS nanoparticles are allowed to settle down at the bottom of the beaker. The higher the particle size, faster is the sedimentation rate.
- **STEP 7:** As soon as the particles are settled at the bottom, the excess solvent is decant to separate out the sedimented particles.
- **STEP 8:** The remaining reactants adhered to the nanoparticles are now washed off by using distilled water and ethanol. For this to be done, a small amount of distilled water is mixed to the settled particles and kept aside until sedimentation process is over. Again, the distilled water is decant and this process is repeated for 3-4 times.
- **STEP 9:** The same step is iterated using ethanol for 3 times. This process ensures purity of the synthesized nanoparticles.
- **STEP 10**: In order to make the ZnO/ZnS nanoparticles dry, the excessive solvent is evaporated. This can be done with the help of a heating mantle where the wet particles are heated to 40°C until the nanoparticles are completely dry and form a layer on the petri dish.
- **STEP 11:** The layer of nanoparticles are scraped off the petri dish using a spatula and are transferred to a mortar. The particles are grinded to a very fine powder with the help of mortar and pestle. The final result is pure form of ZnO/ZnS core-shell nanoparticles which are then characterized and analyzed for various properties.

Synthesis of Cu: ZnO/ZnS Core-Shell Nanoparticles

- **STEP 1:** In this method, copper is first doped on the surface of ZnO core and then encapsulating it with ZnS shell. For this to be done, about 0.18345gof Zinc acetate is added to 50ml of distilled water. Another solution is prepared by adding 0.0018g of copper acetate which act as the dopant in 10ml of ethanol. The above two solutions are mixed together in a 500ml beaker and allowed to stir for 30 minutes at 80°Cusing a magnetic stirrer.
- **STEP 2:** A solution of 0.007g of Sodium hydroxide in 10ml of ethanol is prepared and added dropwise to the stirred solution mixture. It is then allowed to stir for 2-3 hours with temperature being maintained between 60-65°C.
- **STEP 3:** Once the solution is stirred completely, Copper doped ZnO cores are formed which can be capped with ZnS shell.
- **STEP 4:** For the formation of shell, 100 mg of ZnO can be replaced by the above prepared solution containing Cu: ZnO cores which is then mixed with 50ml of isopropanol.
- **STEP 5:** The procedure A is repeated again and the particles are allowed to settle. Excess solvents can be washed off and dried by following the same method as before. Once grinding is done, Cu: ZnO/ZnS nanoparticles are formed with ZnO as core and ZnS as shell which are then studied and analyzed for various properties. The flowchart depicting the entire process of preparation of Cu: ZnO/ZnS core-shell nanoparticles is given below: The pictorial representation of doping Cu on ZnO core is depicted below Figure 3:

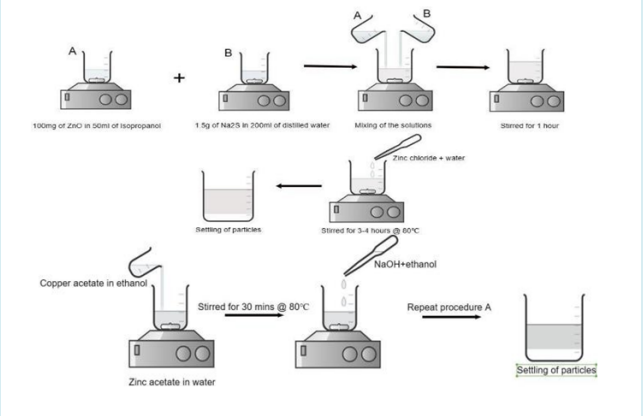

Figure 3: Synthesis procedure of pure and copper doped ZnO@ZnS.

Result and Discussion

XRD Analysis

An X-ray powder diffraction pattern is a plot of the intensity of X-rays scattered at different angles by a sample. The structural properties and characteristics of the synthesized products were determined using powder X- Ray diffraction. The XRD pattern for the as- prepared pure ZnO/ZnS core- shell nanoparticles is shown in Figure 4. Undoped ZnO/ZnS NPs exhibit a total of six intense peaks which are indexed as (111), (100), (002), (101), (102), and (110) respectively. Of these, the peak with (100) plane has the highest intensity at θ value of 15.9257° and with intensity value of 635.69 a.u. It is found that the peak corresponding to (111) plane is due to the presence of ZnS and this indicates the encapsulation of ZnO by ZnS. The pure ZnO/ZnS NPs are also determined to have hexagonal wurtzite structure. The peak intensities of Cu doped ZnO/ZnS NPs is due to defect formation and micro strain effects. The as-prepared NPs are determined to possess hexagonal structure similar to the pure form. Similar to the undoped nanoparticles, Cu doped NPs also show six peaks with a slight variation in peak intensity. The crystalline size of both pure and Cu doped nanoparticles was calculated with the help of Debye-Scherrer equation which is mentioned below:

$$D = K\lambda/\beta\cos\theta \qquad (1)$$

Where D is the crystalline size in nm, K is the shape factor which has the constant value of 0.9, λ is the wavelength of X-ray which is about 1.54 Å, β is full width at half maximum of XRD diffraction peak in radian, θ is Bragg diffraction angle of the peak with high intensity. The value of D for pure core-shell nanoparticles (CSNPs) is calculated to be 42.92 nm and that for ZnO: Cu/ZnS is about 41.5 nm. The decrease in crystalline size for the doped NPs is due to surface and dopant effects. The data obtained for the above calculation is also used for determining the values of micro strain. The formula used for this calculation is given as [9]:

$$\varepsilon = \beta/4\tan\theta \qquad (2)$$

The value of micro strain for pure ZnO/ZnS CSNPs is determined to be $9.66\mu\varepsilon$ and that for ZnO: Cu/ZnS is determined to be $11.04\mu\varepsilon$. The lattice constants a, b and c for pure and doped

NPs are determined using the relation [10]:

$$1/d^2 = 4/3\left(h^2 + hk + k^2/a^2\right) + l^2/c^2 \qquad (3)$$

The determined values lattice constants are a = b = 3.24Å and c = 5.61 Å. The values of a and b are equal due to the fact that the prepared NPs are of hexagonal structure. The lattice constants, crystalline size and other details of both pure and doped nanoparticles are shown in Table 1. The presence of intense sharp peaks ensures the high crystallinity of the synthesized pure and doped NPs.

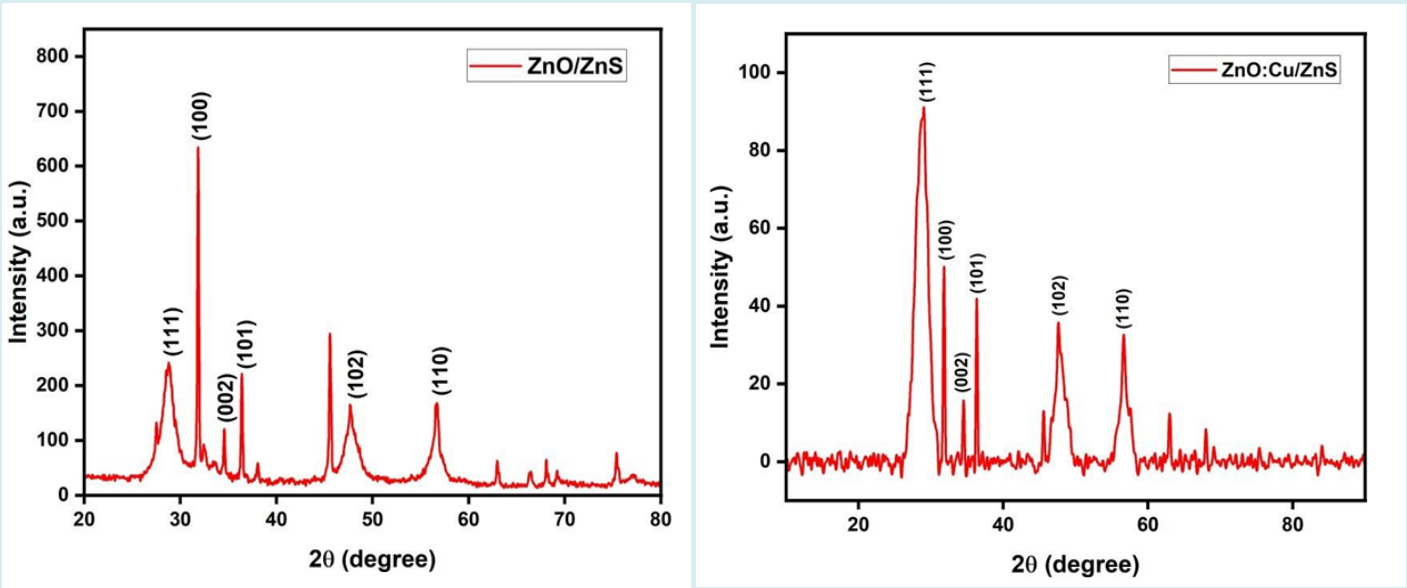

Figure 4: XRD pattern for pure and Cu doped ZnO@ZnS core-shell nanoparticles.

Elements	ZnO/ZnS	ZnO:Cu/ZnS
Crystalline size D (nm)	42.92 nm	41.5 nm
a=b (Å)	3.24 Å	3.24 Å
c (Å)	5.61 Å	5.61 Å
Micro strain (με)	9.66 με	11.04 με
Bandgap energy (eV)	3.15 eV	3.09 eV

Table 1: Index planes, crystalline size, micro strain and lattice constants of pure (ZNO/ZnS) and doped (ZNO: Cu/ZnS) CSNPs.

HRTEM Analysis

HRTEM is the most reliable technique to investigate whether or not the ZnO particles are covered with ZnS. Figure 5 shows the HRTEM images for ZnO:Cu/ZnS CSNPs. From Figure 5 (A-D), the crystalline formation of as- prepared samples can be seen. Figure5 (B) & 5(D) clearly shows the core-shell formation of ZnO: Cu/ZnS CSNPs. Figure 5(E) & 5(F) shows the selected area electron diffraction (SAED) pattern for ZnO:Cu/ZnS CSNPs. This confirms the crystallinity and orientation of lattice points of doped sample. The presence of lattice planes and regular arrangement of lattice points in doped samples can be observed from Figure 6(A) & 6(B). The interplanar spacing, 'd' has also been calculated for the doped samples. The value of d is calculated to be 0.37 nm from Figure 6 (A) and from Figure 6 (B) it is determined as 0.24 nm. From the TEM images, the average crystallite size of pure ZnO was found to be 40 nm. The evaluated crystallite size from the XRD studies, were in good agreement with the TEM results. In Figure 6(A), the corresponding selected area electron diffraction (SAED) pattern indicates the crystallinity and preferential orientation of ZnO samples without any additional diffraction spots of Cu. The HRTEM images show fine crystallinity and clear lattice fringes of pure and Cu doped ZnO with ZnS nanocrystals [11,12].

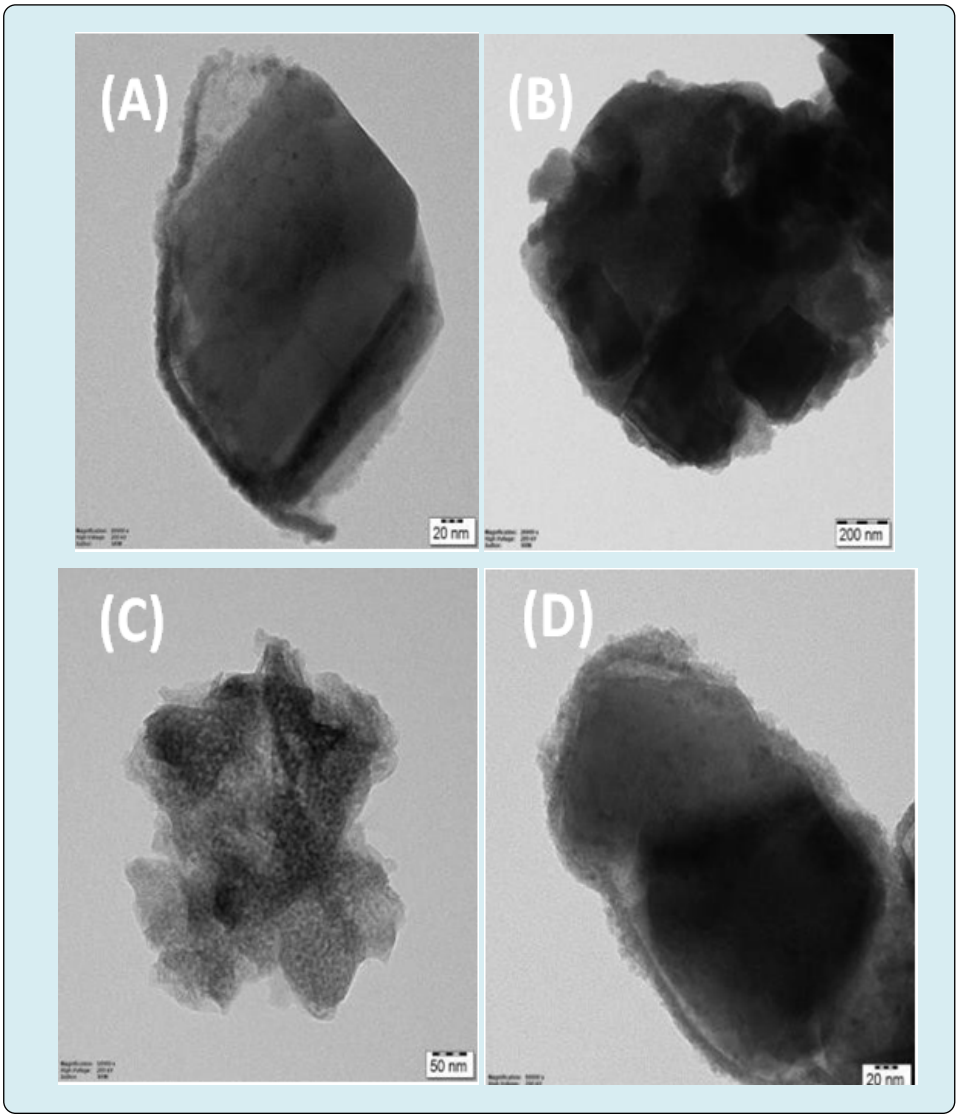

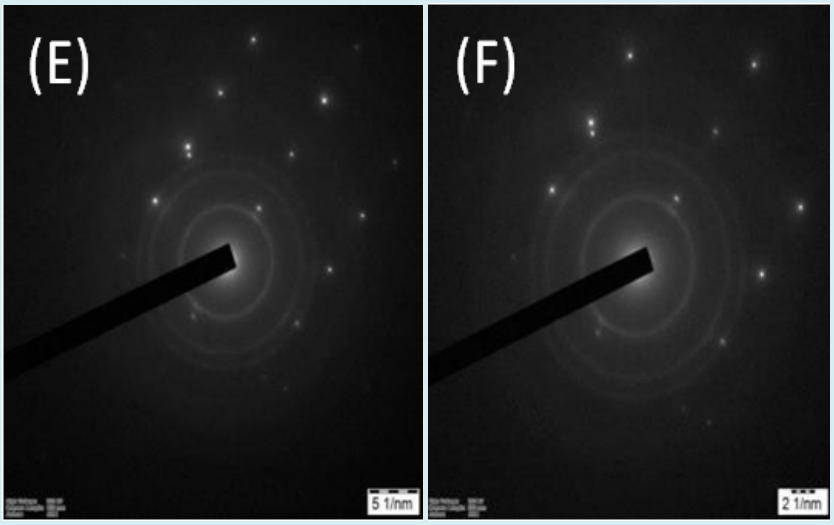

Figure 5: HRTEM images for doped (ZnO:Cu/ZnS) CSNPs.

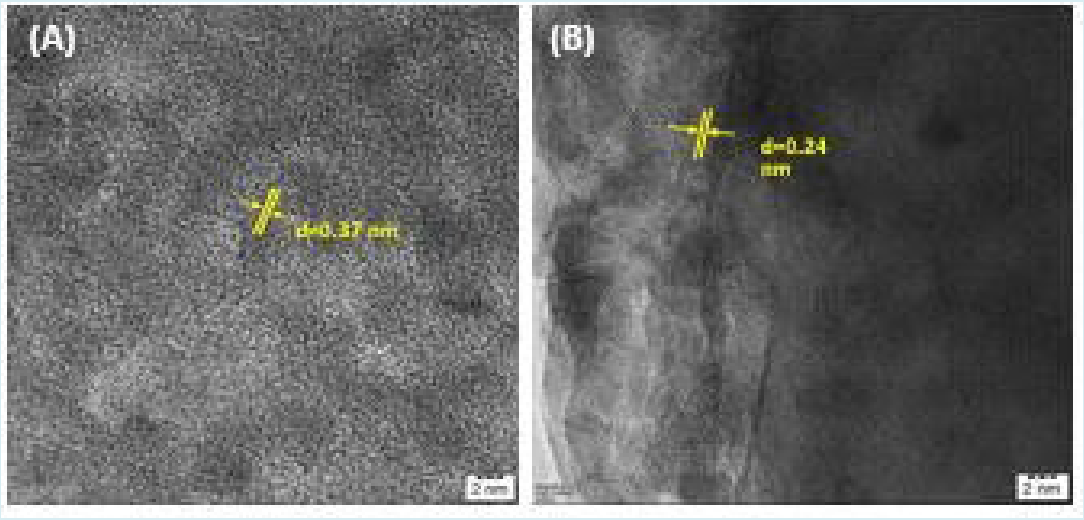

Figure 6: SAED patterns for pure and doped (ZnO:Cu/ZnS) CSNPs.

UV-Vis Absorption Spectra

UV Visible spectroscopy was used to analyze the optical properties and for the calculation of band gap energy for the prepared ZnO/ZnS and ZnO:Cu/ZnS core-shell nanoparticles. Figure 7 shows the absorption spectrum of pure ZnO/ZnS CSNPs. It is seen that the spectrum shows an absorbance peak at wavelength of 318.74 nm which indicates hexagonal wurtzite crystal structure of ZnO/ZnS CSNPs. Figure 7 shows the absorption spectrum of ZnO:Cu/ZnS CSNPs which shows an absorbance peak at 312.26nm. It is also found that the absorption becomes stronger for Cu-doped CSNPs and it is shifted to UV-B region due to the effects of copper doping. The optical band gap energies synthesized NPs were determined from the absorption spectra using Tauc method. The relation between absorption coefficient and band gap energy can be expressed be the following equation [13].

$$(\alpha h\nu)^{\gamma} = A(h\nu - E_g) \quad (4)$$

Here α is the absorption coefficient which has a constant value of 2.302(A/t), A is the absorbance value which is determined from the plot and Eg is the band gap energy to be calculated. The value of γ = 2 for the direct band gap of the NPs. An extrapolation of the linear region of a plot of (αhν) 2 versus photon energy (hν) curve on the energy axis gives the value of the optical band gap (Eg). Figure 8 show the band gap energies of pure and Cu-doped CSNPs. The calculated

band gap energy for pure CSNPs was about 3.15eV. Similarly, the band gap energy for ZnO:Cu/ZnS CSNPs was calculated as 3.09 eV. It can be observed that there is a slight decrease in the Eg value of copper doped CSNPs [14]. This is due to combination of quantum confinement and the presence of defects and strains induced by copper doping. It may also be noted that the electrical conductivity of Cu-doped CSNPs has been enhanced since there is decrease in its band gap energy [15]. The below table 2 shows the wavelength of maximum absorbance and band gap energies for ZnO/ZnS and ZnO:Cu/ZnS CSNPs:

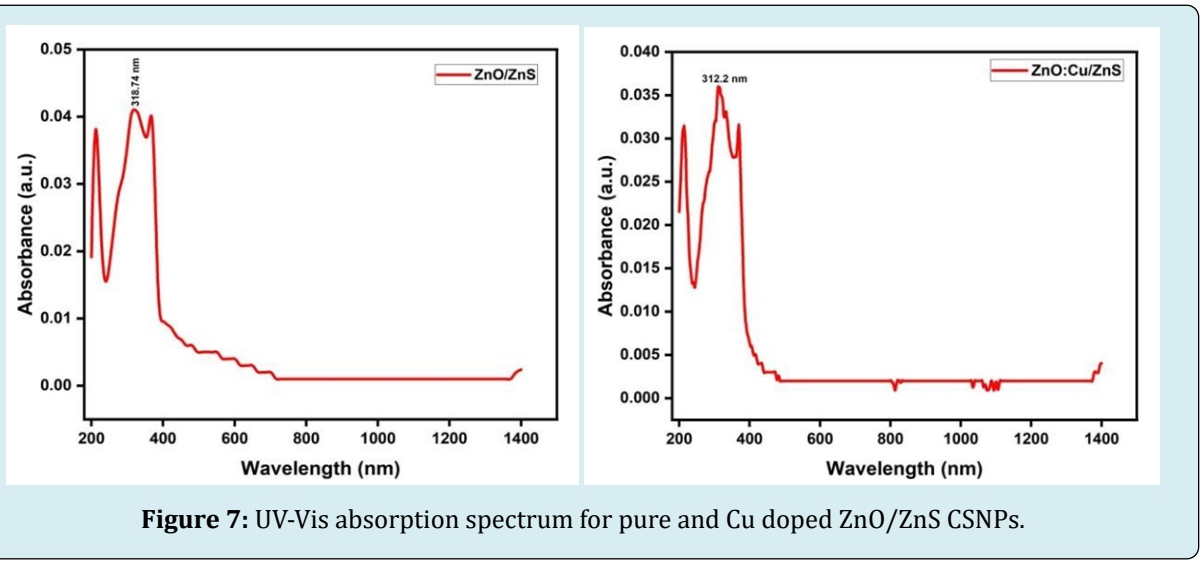

Figure 7: UV-Vis absorption spectrum for pure and Cu doped ZnO/ZnS CSNPs.

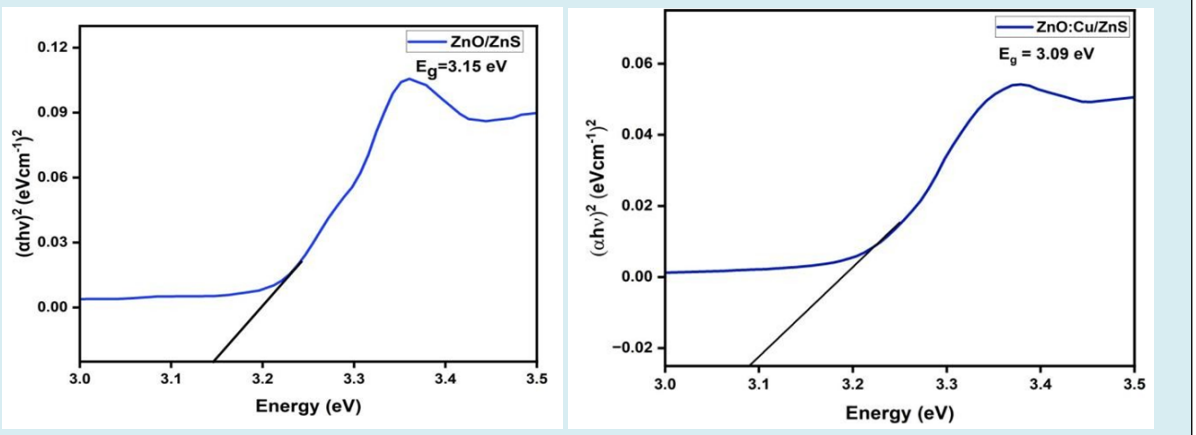

Figure 8: Band gap energy for pure and Cu doped (ZnO/ZnS) CSNPs.

Elements	ZnO/ZnS	ZnO:Cu/ZnS
Wavelength (nm)	318.74 nm	312.26 nm
Bandgap energy (eV)	3.15 eV	3.09 eV

Table 2: Elemental (nm, eV) values of ZnO/ZnS, ZnO: Cu/ZnS.

FT-IR Analysis

The optical characteristics and chemical bonding of the synthesized nanoparticles were studied using Fourier Transform Infrared (FT-IR) spectroscopy. Room-temperature FT-IR spectra for both pure and copper-doped ZnO/ZnS core-shell nanoparticles (CSNPs) were recorded over the wavenumber range of 1000 to 4000 cm^{-1}. Figure 9 presents the FT-IR spectra for the pure ZnO/ZnS CSNPs, where several characteristic peaks are observed, indicating the presence of specific functional groups and chemical bonds. The stretching vibration of the Zn–O bond, a signature of the ZnO core, is identified at around 430 cm^{-1}, confirming the presence of zinc oxide within the core-shell structure. The strong peak at 3320.1 cm^{-1} corresponds to the stretching vibrational mode of O–H bonds, indicating the presence of hydroxyl groups [16]. This hydroxyl group is common in nanoparticle synthesis, often arising due to surface-adsorbed water or

hydroxyl species on the nanoparticle surface. Additionally, the bending vibration of the hydroxyl O–H bond is evident from the peak at 1629.95 cm^{-1}, while the peak at 1435 cm^{-1} further ensures the presence of O–H–O bonds, confirming residual water content or surface hydroxylation [17].

At 1108.7 cm^{-1}, the FT-IR spectrum indicates the presence of C–C bonds, and this peak also suggests the ZnS shell's successful formation, ensuring the ZnO core is encapsulated by ZnS [18]. The various vibrational modes and corresponding bond assignments for pure ZnO/ZnS CSNPs are summarized in Table 3. The FT-IR spectra for the copper-doped ZnO/ZnS nanoparticles are also shown in Figure 9, where similar peaks are observed, with slight shifts in their wavenumbers due to the effects of copper doping. For the doped nanoparticles, the O–H stretching vibration is present at 3266.75 cm^{-1}, confirming the persistence of hydroxyl groups. The bending vibration of the O–H bond appears at 1621.06 cm^{-1}, indicating a slight shift compared to the undoped sample, which is likely caused by strain and defects introduced by copper incorporation into the ZnO lattice [19]. Additionally, the C–C bond, which confirms the presence of the ZnS shell and some organic residues, is observed at 1092.33 cm^{-1}. The slight shifts in the wavenumbers and peak intensities in the copper-doped sample can be attributed to the strain effects induced by copper doping. Copper doping typically introduces lattice distortions, affecting the vibrational frequencies of the bonds in the material. This strain is also likely responsible for slight changes in the FT-IR spectra compared to the pure ZnO/ZnS CSNPs [20].

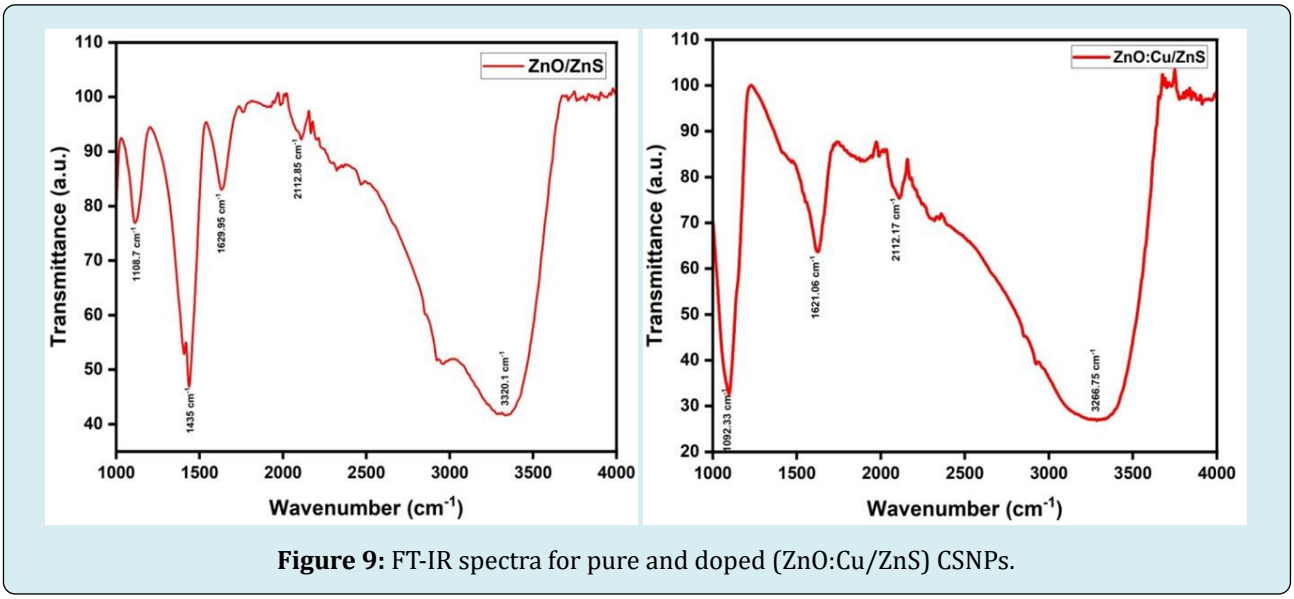

Figure 9: FT-IR spectra for pure and doped (ZnO:Cu/ZnS) CSNPs.

Wavenumbers (cm^{-1})	Chemical bonds
430 cm^{-1}	Zn-O bond
3320.1 cm^{-1}	O-H bond (stretching)
1629.95 cm^{-1}	O-H bond (bending)
1435 cm^{-1}	O-H-O bond
1108.7 cm^{-1}	C-C bond

Table 3: Different chemical bonds based on wavenumbers.

Photoluminescent Analysis

The optical properties of pure and copper-doped ZnO/ZnS core-shell nanoparticles (CSNPs) were studied through photoluminescence (PL) spectroscopy. PL spectroscopy is a powerful technique to assess the emission characteristics of materials, especially in nanostructures where quantum confinement effects can significantly alter their optical properties. The PL spectra of the as-prepared pure ZnO/ZnS CSNPs and copper-doped ZnO/ZnS CSNPs are presented in Figure 10.

From the spectra, it is evident that the pure ZnO/ZnS CSNPs exhibit a strong emission peak centered around 400 nm in the UV region. This emission peak corresponds to the near-band- edge (NBE) emission of the ZnO core. ZnO has a direct band gap, and its typical excitonic emission occurs in the ultraviolet region due to the recombination of free excitons in the conduction and valence bands [21]. In the case of pure ZnO/ZnS CSNPs, the band gap energy was calculated to be approximately 3.2 eV for a wavelength of 380.42 nm. This value is consistent with the known band gap energy of ZnO, confirming the successful formation of the ZnO core structure. For the copper-doped ZnO/ZnS CSNPs, a significant shift in the emission wavelength is observed. The PL spectrum shows a strong emission peak around 500 nm in the visible region. This shift in the emission wavelength can be attributed to the incorporation of copper (Cu) ions

into the ZnO lattice [22]. Copper ions act as impurities, introducing defect states within the band structure of ZnO. These defect states trap electrons and holes, altering the recombination process and resulting in emission at longer wavelengths. The band gap energy for ZnO/ZnS CSNPs was calculated to be approximately 3.3 eV. The slight increase in band gap energy compared to pure ZnO/ZnS CSNPs suggests that copper doping not only introduces new defect states but also slightly modifies the electronic structure of the material [23].

The stronger PL emission from both the pure and copper-doped CSNPs provides confirmation of the successful capping of ZnS over the ZnO core, leading to the formation of the core-shell structure. ZnS serves as a passivation layer, reducing surface defects and enhancing the emission properties of the ZnO core. The presence of the ZnS shell likely plays a critical role in improving the overall optical stability of the nanoparticles, as it helps reduce non-radiative recombination processes that would otherwise quench the PL emission [24]. A notable observation is the increased peak intensity in the PL spectrum of copper-doped ZnO/ZnS CSNPs compared to the pure ZnO/ZnS CSNPs. This increase suggests that the incorporation of copper significantly enhances the optical properties of the nanoparticles. The Cu ions, acting as luminescent centers, introduce energy levels within the band gap that facilitate radiative recombination, thus enhancing the emission intensity [25]. This result indicates that copper doping not only modifies the emission wavelength but also boosts the overall luminescence efficiency of the CSNPs.

Thus, the optical investigations of pure and copper-doped ZnO/ZnS CSNPs using PL spectroscopy reveal distinct emission characteristics for each type of nanoparticle. The pure ZnO/ZnS CSNPs exhibit strong UV emission due to near-band- edge excitonic recombination, while the copper-doped ZnO/ZnS CSNPs show visible emission, attributed to the defect states introduced by Cu doping [26]. The enhanced peak intensity for the doped nanoparticles confirms that copper doping effectively improves the optical properties, making these nanoparticles promising for applications in optoelectronic devices and luminescent materials.

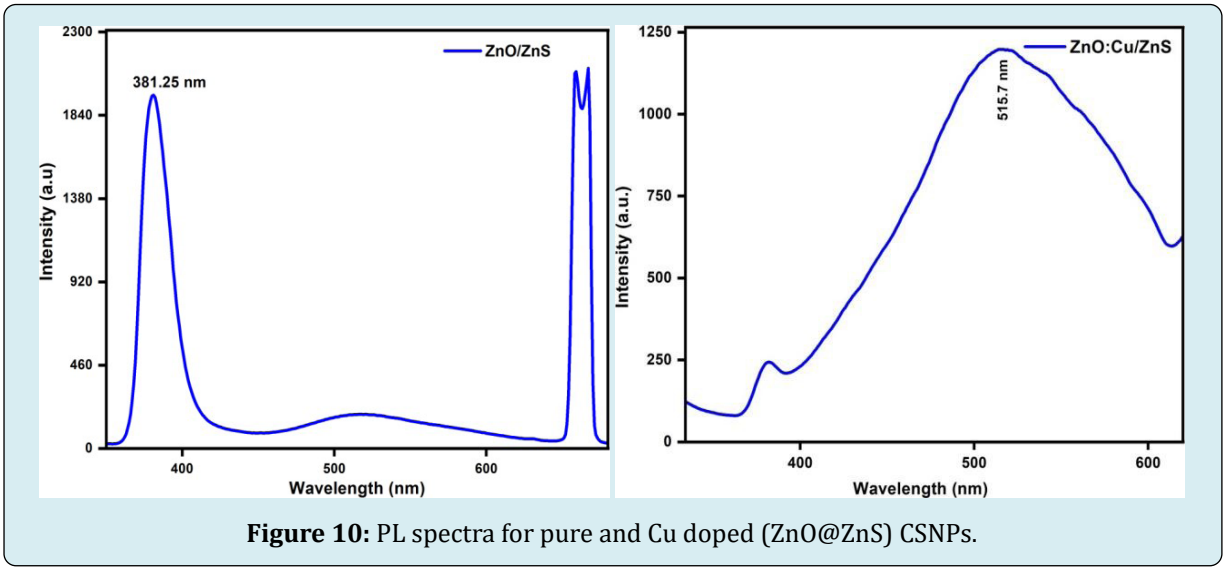

Figure 10: PL spectra for pure and Cu doped (ZnO@ZnS) CSNPs.

VSM Analysis

Vibrating Sample Magnetometer was used to study and analyse the magnetic properties of the CSNPs. Figure 11 shows the M-H curve for pure ZnO/ZnS core-shell nanoparticles. The saturation magnetization (Ms) of pure CSNPs was found to be 30.86 emu and its retentivity was determined to have the value of 2.47 emu. The value of remanent magnetization (Mr) was determined as 1.35 emu/g and the value of coercive field is around-603.92Oe. Figure 11 shows the M-H curve for doped ZnO:Cu/ZnS CSNPs. Similar to the pure form, the saturation magnetization (Ms) was determined to be 34.09 emu and the value of retentivity was found as 1.59 emu. The remanent magnetization (Mr) was found to have the value of -1.182 emu/g and that of the coercive field was around -255.52 Oe. Both the pure and doped forms show ferromagnetic properties. The pure CSNPs have considerably low saturation magnetization values than that of dopes ones. The narrow loop of Cu-doped CSNPs shows that it act as soft ferromagnets whereas the pure forms act as hard ferromagnets [27]. The value sof remanent magnetization and corresponding retentivity of ZnO:Cu/ZnS CSNPs are smaller than pure CSNPs which indicates that Cu-doped CSNPs retain smaller magnetic properties than the pure ones when the external magnetic field is removed. This ensures that ZnO:Cu/ZnS CSNPs cannot be used as permanent magnets and can be magnetized when an external magnetic field is applied to them. Meanwhile, the pure forms can retain

its magnetic properties to a larger extent which indicates that they can be used as permanent magnets [28]. In addition to these, it is also evident that the loop of pure forms is wider than the loop of Cu-doped ones. This ensures that ZnO/ZnS CSNPs are hard ferromagnetic materials and ZnO: Cu/ZnS CSNPs are soft ferromagnetic materials [29,30]. The table 4 showing the parameters determined from the M-H curve for both pure and doped CSNPs is given below:

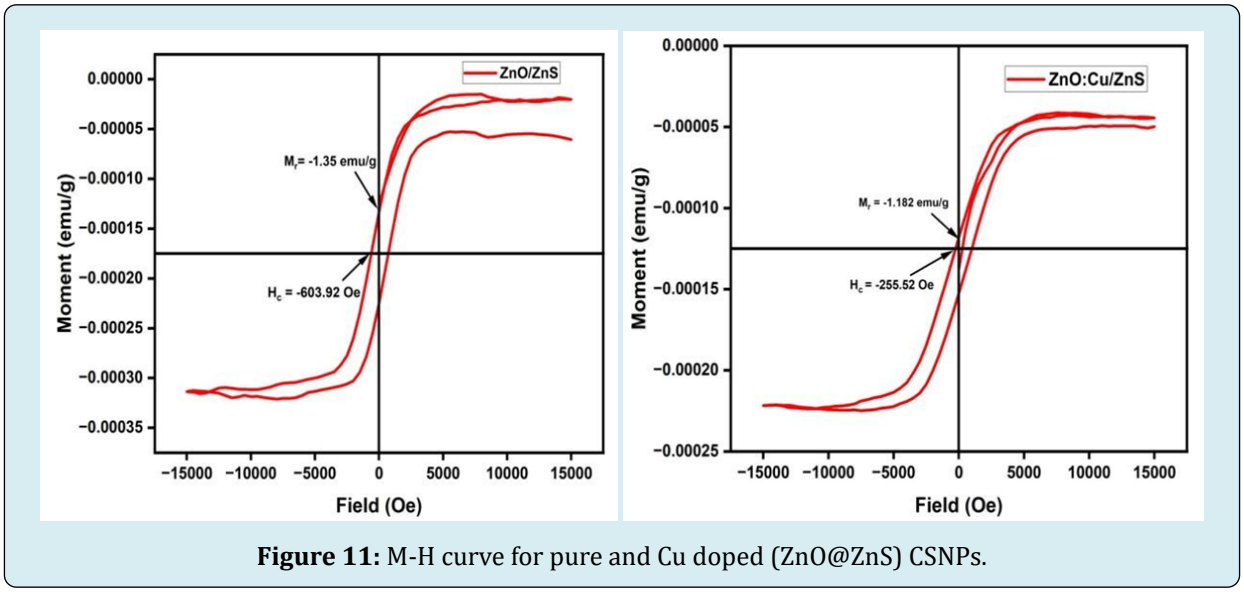

Figure 11: M-H curve for pure and Cu doped (ZnO@ZnS) CSNPs.

Parameters	ZnO/ZnS	ZnO:Cu/ZnS
Saturation magnetization (Ms)	30.86 emu/g	34.09 emu/g
Remanent magnetization (Mr)	-1.35 emu/g	-1.182 emu/g
Coercivity (Hc)	-603.92 Oe	-255.52 Oe
Retentivity	2.47 emu	1.59 emu

Table 4: Different parameter values for ZnO/ZnS & ZnO:Cu/ZnS.

Biological Application

Copper-doped ZnO/ZnS core-shell nanoparticles (CSNPs) have emerged as promising candidates for various biological applications due to their enhanced optical, antibacterial, and catalytic properties. The incorporation of copper into the ZnO core significantly boosts their photoluminescence, particularly in the visible spectrum, making these nanoparticles ideal for bioimaging and biosensing. The strong fluorescence of Cu- doped ZnO/ZnS CSNPs allows them to act as efficient probes for high-resolution imaging of biological systems, facilitating better visualization of cells and tissues [31]. Their ability to provide clear and sustained emission signals is crucial for accurate imaging in complex biological environments. Moreover, Cu-doped ZnO/ZnS CSNPs demonstrate notable antibacterial activity, primarily due to the combined effects of zinc oxide and copper ions. Copper ions have been widely studied for their antimicrobial properties, which arise from their capacity to generate reactive oxygen species (ROS) and disrupt bacterial cell membranes, leading to cell death [32]. This makes these nanoparticles particularly useful for developing antimicrobial coatings, wound dressings, and medical devices where sterilization is critical. Their strong bactericidal activity against pathogens such as *E. coli* and *S. aureus* further underscores their potential in healthcare settings [33]. In drug delivery applications, Cu-doped ZnO/ZnS CSNPs offer versatility due to their core-shell structure, which provides a protective encapsulation for therapeutic agents [34]. Functionalization of the ZnS shell allows for targeted delivery, while controlled release can be triggered by external stimuli such as pH changes or light exposure. This capability makes them suitable for delivering drugs in a more controlled manner to specific sites in the body, enhancing the efficacy of treatment while minimizing side effects [35]. Thus, copper-doped ZnO/ZnS CSNPs represent a versatile and multifunctional nanomaterial with significant potential in biomedicine, including diagnostics, antimicrobial therapies, and drug delivery systems (Figure 12) [36].

Figure 12: Different types of ZnO@ZnS Core Shell Nanoparticles.

Conclusion

Pure ZnO/ZnS and doped ZnO: Cu/ZnS core-shell nanoparticles were synthesized by chemical methods. ZnO cores were first prepared by an effective co-precipitation method and then covered with ZnS by chemical method in just two steps at low temperature. ZnO: Cu/ZnS were also synthesized by following the same methods except for the difference where Copper acetate is used as the doping agent. It is seen that doping CSNPs with copper enhances its optical, magnetic and electrical properties. Powder XRD was performed for analyzing the structural properties of the so- prepared CSNPs. The crystalline size (D) of pure CSNPs was determined using XRD as 42.92 nm and that for copper doped CSNPs was 41.5 nm. The values of micro strain for pure and doped CSNPs were 9.66 με and 11.04 με. From XRD data, the lattice constants for both pure and doped CSNPs were calculated as a = b = 3.24 Å and c = 5.61 Å. The optical properties of the prepared nanoparticles were studied using UV-Vis, FT-IR and PL spectra. The band gap energy for ZnO/ZnS CSNPs has been determined to be 3.15eV and for ZnO: Cu/ZnS has been determined to have band gap energy of 3.09 eV. This calculation was performed with the help of respective UV-Vis and PL spectra. Thus, copper doped CSNPs have enhanced optical, electrical properties and better conductivity, since its band gap energy has been decreased. From FT-IR spectra of pure and doped forms, the chemical bonds and their modes of vibrations has been determined. The presence of stretching and bending hydroxyl O-H bonds, O-H-O bonds, Zn-O bonds and C-C bonds in ZnO/ZnS and ZnO: Cu/ZnS were confirmed by their FT-IR spectra. From the spectral analysis, the capping of ZnS shell over ZnO core was also assured. The variation of peaks of cu-doped CSNPs may be due to dopant effects and surface effects.

The introduction of copper ions into the crystal lattice can affect the arrangement of atoms which results in lattice strain and distortion. It may also influence the surface diffusion, thus leading to reduced crystallite size of the doped CSNPs. Thus ZnO/ZnS and ZnO: Cu/ZnS can be employed to enhance the optical properties of semiconductors and photodiodes and can be effectively used in quantum computing, drug delivery, solar cells and various other fields.

Conflict of Interest

The authors declare that there is no conflict of interest.

Acknowledgements

The author expresses gratitude to B.S. Abdur Rahman Crescent Institute of Science and Technology for their financial support, specifically referencing the grant number Ref: CSD/SMPS/2024/P2/21. This support has significantly contributed to the author's work and research endeavors.

References

1. Ealia S, Mary A, Saravanakumar MK (2017) A review on the classification, characterisation, synthesis of

nanoparticles and their application. In: IOP conference series: materials science and engineering, IOP Publishing 263(3): 032019.

2. Lu HY, Chu SY, Tan SS (2004) The characteristics of low-temperature-synthesized ZnS and ZnO nanoparticles. Journal of Crystal growth 269(2-4): 385-391.

3. Sookhakian M, Amin YM, Basirun WJ, Tajabadi MT, Kamarulzaman N (2014) Synthesis, structural, and optical properties of type-II ZnO–ZnS core–shell nanostructure. Journal of Luminescence 145: 244-252.

4. Sadollahkhani A, Kazeminezhad I, Lu J, Nur O, Hultman L, et al. (2014) Synthesis, structural characterization and photocatalytic application of ZnO@ ZnS core–shell nanoparticles. RSC advances 4(70): 36940-36950.

5. Jing D, Li R, Liu M, Guo L (2011) Copper-doped ZnO/ZnS core/shell nanotube as a novel photocatalyst system for photocatalytic hydrogen production under visible light. International journal of nanotechnology 8(6-7): 446-457.

6. Haider J (2021) Synthesis, characterization and antibacterial activity of simple ZnO and metal doped ZnO nanoparticles. Pak J Pharm Sci 34(5): 1651-1658.

7. Karthik KV, Raghu AV, Reddy KR, Ravishankar R, Sangeeta M, et al. (2022) Green synthesis of Cu-doped ZnO nanoparticles and its application for the photocatalytic degradation of hazardous organic pollutants. Chemosphere 287: 132081.

8. Demirbilek N, Yakuphanoğlu F, Kaya M (2021) Structural and optical properties of pure ZnO and Al/Cu co-doped ZnO semiconductor thin films and electrical characterization of photodiodes. Materials Testing 63(3): 279-285.

9. Rajiv P, Rajeshwari S, Venckatesh R (2020) Synthesis and characterization of copper- doped ZnO nanoparticles and its application for antibacterial activity. Spectrochimica Acta Part A: Molecular and Biomolecular Spectroscopy 118(7): 203-207.

10. Murali G, Ganesan R, Sathyamoorthy R (2018) Effect of copper doping on the structural and optical properties of ZnO nanoparticles synthesized by coprecipitation method. Materials Science in Semiconductor Processing 90(4): 87-94.

11. Karar N (2007) Photoluminescence from doped ZnS nanostructures. solid state communications 142(5): 261-264.

12. Rouhi J, Ooi CR, Mahmud S, Mahmood MR (2015) Synthesis of needle-shape ZnO-ZnS core-shell heterostructures and their optical and field emission properties. Electronic Materials Letters 11: 957-963.

13. Sivasankari J, Sankar S, VimalaDevi L (2015) Influence of doping group I elements on structural, optical and magnetic properties of nanocrystalline ZnO. Journal of Materials Science: Materials in Electronics 26: 8089-8096.

14. Kumar V, Bharti D, Nagarajan R (2020) Optical and electrical properties of Cu-doped ZnO nanoparticles. Journal of Alloys and Compounds 836(2): 155486.

15. Singh M, Jain R, Kumar A (2021) Quantum confinement and optical properties of Cu- doped ZnO/ZnS core-shell nanostructures. Journal of Physics D: Applied Physics 54(13): 135301.

16. Pattanayak DK, Nayak P (2021) Structural and FTIR analysis of ZnO nanoparticles synthesized via the green route. Journal of Materials Science: Materials in Electronics 32(5): 10101-10109.

17. Ramasamy P, Kim B, Lee J (2020) Structural, optical, and photocatalytic properties of ZnO/ZnS core/shell nanoparticles synthesized by a facile hydrothermal method. Journal of Nanomaterials 2020: 4056392.

18. Tiwari N, Chauhan NPS, Singh P (2019) Cu-doped ZnO nanoparticles: Structural, optical and FTIR studies. Journal of Materials Science Materials in Electronics 30(13): 11604-11615.

19. Suresh R, Kumar S, Ponnusamy S (2018) Optical, structural, and FTIR studies of Cu- doped ZnO nanostructures synthesized by sol-gel method. Journal of Nanostructure in Chemistry 8(4): 383-391.

20. Kumar P, Sharm V, Jain R (2021) FTIR analysis and structural characterization of ZnO and Cu doped ZnO nanoparticles. Journal of Physics D Applied Physics 54(9): 093301.

21. Norek M (2019) Approaches to enhance UV light emission in ZnO nanomaterials. Current Applied Physics 19(8): 867-883.

22. Xu CX, Sun XW, Zhang XH, Ke L, Chua SJ (2004) Photoluminescent properties of copper- doped zinc oxide nanowires. Nanotechnology 15(7): 856.

23. Khodamorady M, Bahrami K (2023) Fe_3O_4@BNPs@ZnO–ZnS as a novel, reusable and efficient photocatalyst for dye removal from synthetic and textile wastewaters. Heliyon 9(6).

24. Mehta SK, Kumar S (2010) Influence of surfactant structures in luminescence enhancement dynamics during nucleation and growth of aqueous ZnS nanoparticles and their photoactivation due to illumination with UV/visible light. Journal of luminescence 130(12): 2377-2384.

25. Raji R, Gopchandran KG (2017) ZnO: Cu nanorods with visible luminescence: copper induced defect levels and its luminescence dynamics. Materials Research Express 4(2): 025002.

26. Sun Y, Zhang W, Li Q, Liu H, Wang X (2023) Preparations and applications of zinc oxide based photocatalytic materials. Advanced Sensor and Energy Materials 2(3): 100069.

27. Sokovnin S, Ilves V (2023) Nanopowders of Metal Oxides and Fluorides: Preparation, Properties, and Applications. Jenny Stanford Publishing, pp: 750.

28. Leslie-Pelecky DL, Rieke RD (1996) Magnetic properties of nanostructured materials. Chemistry of materials 8(8): 1770-1783.

29. Nur O, Willander M (2019) Low temperature chemical nanofabrication: recent progress, challenges and emerging technologies. Micro and Nano Technologies pp: 246.

30. Kaushik A, Dalela B, Rathore R, Vats VS, Choudhary BL, et al. (2013) Influence of Co doping on the structural, optical and magnetic properties of ZnO nanocrystals. Journal of alloys and compounds 578: 328-335.

31. Manzoor M, Ahmad M, Ahmad S, Firdous A (2021) Copper-doped ZnO nanostructures for biomedical and environmental applications. Ceramics International 47(2): 2903-2910.

32. Khan I, Saeed K, Khan I (2019) Nanoparticles: Properties, applications and toxicities. Arabian Journal of Chemistry 12(7): 908-931.

33. Chowdhury U, Mandi P, Mukherjee R, Chandra S, Sutradhar S, et al. (2024) Dual Self-Referenced Refractive Index Sensor Utilizing Tamm Plasmons in Photonic Quasicrystal for Multistage Malaria Parasite Detection. Plasmonics pp: 1-13.

34. Chatterjee S, Mukherjee R, Chandra S, Maity AR, Kumar S, et al. (2024) Harnessing Tamm-Plasmon Polaritons in Cantor Sequence Photonic Quasicrystals for Enhanced Cancer Cell Detection. Plasmonics pp: 1-12.

35. Bharti D, Kumar V, Nagarajan R (2020) Antimicrobial activities of Cu-doped ZnO nanoparticles and its role in photocatalytic degradation of organic dyes. Journal of Materials Science Materials in Electronics 31(12): 1-12.

36. Kalashgarani MY, Babapoor A (2022) Application of nano-antibiotics in the diagnosis and treatment of infectious diseases. Adv Appl Nano Bio Technol 3(1): 22-35.